Dependence of Counterion Binding on DNA Shape as Determined By Counterion Condensation Theory

Marcia O. Fenley,*,† Wilma K. Olson, and Gerald S. Manning*

Department of Chemistry, Rutgers University, 610 Taylor Road, Piscataway, New Jersey 08854-8087, and Department of Physics, Campus Box 1105, One Brookings Drive, Washington University, St. Louis, Missouri 63130

Received February 10, 1999; Revised Manuscript Received November 12, 1999

ABSTRACT: We have computed the fraction of DNA phosphate charge neutralized by condensed counterions for parallel pairs of linear DNA segments, DNA circles, and representative closed-circular supercoiled DNA configurations ranging in length from 42 to 3000 base pairs. We find significant but small uptake of condensed counterions for the more compact structures relative to an isolated linear DNA segment.

1. Introduction

Gel electrophoresis measurements of the extent of DNA phosphate charge neutralization by the cations of mixed salt solutions (e.g., the Mg^{2+} and Na^+ ions in $MgCl_2$/NaCl solution) have been reported.[1−4] An interesting observation is that the neutralization fractions of a circularized supercoiled DNA and its linear counterpart are not significantly different.[1] Since both curvature within a segment and juxtaposition of distant segments are enhanced by supercoiling, the phosphate charge density must be greater in at least some regions of supercoiled DNA than in linear DNA. One might then have expected an uptake of additional neutralizing counterions when linear DNA is circularized and supercoiled. In fact, counterion condensation theory predicts that when two line charges approach in parallel, the fractional neutralization by univalent counterions increases from the value $1 - \xi^{-1}$ at far distances to $1 - (2\xi)^{-1}$ at close distances.[5] Here, ξ is a dimensionless measure of the charge density of a single line charge (the ratio of the Bjerrum length to the charge spacing on the line), so the meaning is that two close line charges are neutralized to the same extent as a single line charge of twice the charge density. Since $\xi = 4.2$ for linear B-form DNA, the numerical prediction is that DNA phosphate charge neutralization by bound Na^+ ions increases from 0.76 for an isolated DNA segment to 0.88 for two sufficiently close parallel segments. This difference would be easily detected by the highly precise gel electrophoresis experiment.

The neutralization fractions obtained from the gel measurements for both linear and supercoiled DNA were found[1−3] to be in quantitative agreement with the predictions of analytical two-variable counterion condensation theory, designed for linear DNA (or any linear polyion) in mixed salts.[6] The agreement of theory and experiment suggests that both valence types of counterion present in the mixture bind in reality as in the theory—in a delocalized manner.[6] To understand why the theory for linear DNA also works when applied to data for supercoiled DNA, we have calculated and report here the extent of phosphate neutralization by condensed counterions for a wide variety of DNA shapes, as predicted by a numerical version of counterion condensation theory that retains the picture of delocalized binding but is not restricted to rodlike configurations.[7]

Many experimental and theoretical studies have shown that the spatial configuration of supercoiled B-DNA is affected by changes in the ionic strength of the solution.[8−17] An increased ionic strength causes a shift from a relatively open to a relatively compact shape. We will try to address the question of whether a significant uptake of condensed counterions accompanies an open to compact conformational transition. Recall that an ionic strength increase in the range of typical values does not lead to an increase in the number of counterions condensed on linear polyions.[18,19]

Among our results are calculated neutralization fractions for pairs of approaching line segments and for circular arcs. In the latter case, we extend results previously reported.[20] In both cases we find qualitative similarity to Fixman's Poisson−Boltzmann treatment.[21] It should be noted, however, that in the context of Poisson−Boltzmann theory some criteria for classifying counterions as neutralizing and not neutralizing may be more satisfactory than others.[19]

2. DNA Representation and Numerical Method

We consider lines, circles, and various closed-circular supercoiled configurations of B-DNA with one charged phosphate group on every nucleotide residue. In the case of linear DNA, the double helical array of phosphate groups is represented by a linear sequence of charges in place of the phosphate groups. Each phosphate group is reduced to a point charge centered at the axial projection of the phosphorus atom and sequential charges are placed 1.7 Å apart along the chain contour, i.e., two phosphate groups per 3.4 Å base-pair step. This spacing differs from the nonuniform spacing of phosphates along the axis of the canonical B-DNA fiber diffraction model[22] (1.2 Å between charges of complementary residues and 2.2 Å between charges of sequential residues) and the displacement of phosphorus atoms seen in B-DNA crystals.[23] The supercoiled shapes treated in Figures 1 and 2 are based on the exact solutions of the equations of equilibrium of an ideal (359

* To whom correspondence should be addressed. E-mail: fenley@hbar.wustl.edu; gmanning@rutchem.rutgers.edu.
† Washington University.

10.1021/ma990191u CCC: $19.00
Published on Web 02/05/2000

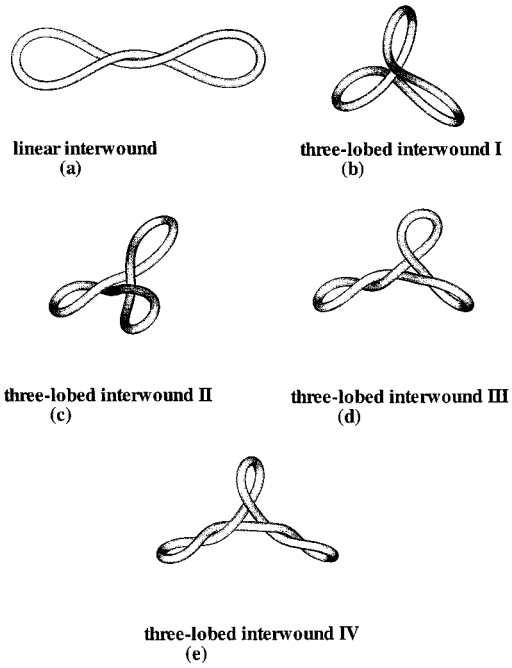

Figure 1. Different elastic equilibrium supercoiled configurations of 359 bp DNA miniplasmids. These structures were obtained from exact solutions of the Kirchoff equations of equilibrium for elastic rods of circular cross section, which account for effects of impenetrability and self-contact forces (see ref 24). The bending constant is fixed at 2.058×10^{-19} erg cm (which corresponds to a persistence length of 500 Å at 298 K), $C/A = 1.5$ (where C is the torsional rigidity constant), and the effective diameter of DNA is set to 20 Å. The equilibrium supercoiled configurations shown in panels a−e have the following characteristics: (a) $\Delta Lk = 2.51$, $n = 3$, $Wr = 2.06$, $R_g = 163.8$ Å, $\langle P-P \rangle = 195.8$ Å; (b) $\Delta Lk = 1.79$, $n = 3$, $Wr = 1.95$, $R_g = 108.7$ Å, $\langle P-P \rangle = 138.9$ Å; (c) $\Delta Lk = 3.97$, $n = 3$, $Wr = 2.80$, $R_g = 112.2$ Å, $\langle P-P \rangle = 144.3$ A; (d) $\Delta Lk = 4.00$, $n = 5$, $Wr = 3.13$, $R_g = 116.4$ Å, $\langle P-P \rangle = 144.3$ Å; (e) $\Delta Lk = 5.02$, $n = 7$, $Wr = 3.86$, $R_g = 117.0$ Å, $\langle P-P \rangle = 144.5$ Å. ΔLk is the linking number relative to relaxed DNA, n is the number of self-contacts at 20 Å, Wr is the writhing number, R_g is the radius of gyration, and $\langle P-P \rangle$ is the average interphosphorus distance. The images were generated by the graphics program Tecplot.

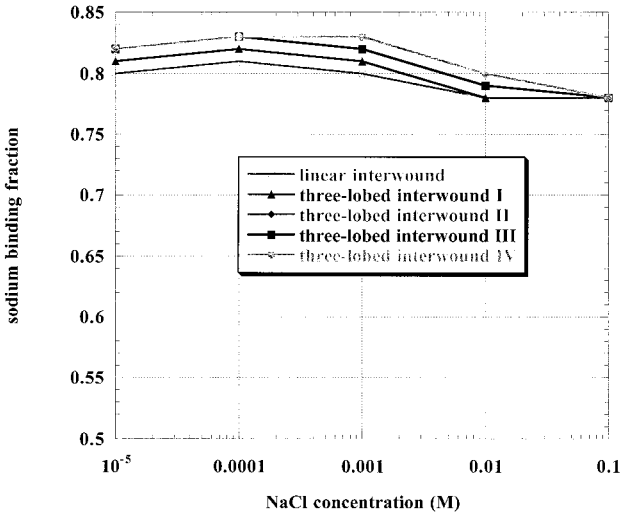

Figure 2. Sodium binding fraction θ of different equilibrium supercoiled configurations of a 359 bp DNA miniplasmid (shown in Figure 1) as a function of NaCl concentration.

bp) elastic DNA rod subject to self-contact.[24] Negative point charges are evenly spaced along the axes of the

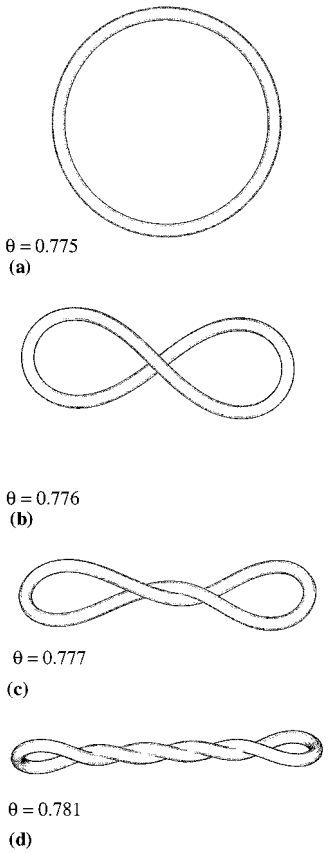

Figure 3. Sodium binding fraction θ of equilibrium configurations of a 1000 bp DNA plasmid in a 0.1 NaCl aqueous solution at different ΔLk. These equilibrium configurations of closed-circular DNA were obtained from numerical solutions of elastic theory equations which acount for long-range self-contact forces (see ref 25). The bending and twisting constants are fixed at 1.3×10^{-19} erg cm (persistence length 310 Å) and 1.0×10^{-19} erg cm, respectively. The structures shown in panels a−d have the following characteristics: (a) $\Delta Lk = 0$, $Wr = 0$, $R_g = 537.9$ Å, $\langle P-P \rangle = 627.0$ Å; (b) $\Delta Lk = -2$, $d = 55.6$ Å, $Wr = -0.95$, $R_g = 442.5$ Å, $\langle P-P \rangle = 477.3$ Å; (c) $\Delta Lk = -4$, $d = 50.0$ Å, $Wr = -2.09$, $R_g = 453.1$ Å, $\langle P-P \rangle = 474.1$ Å; $\Delta Lk = -6$, $d = 41.7$ Å, $Wr = -3.63$, $R_g = 459.2$ Å, $\langle P-P \rangle = 468.8$ Å. d is the distance of closest approach, and the other symbols are defined in the caption to Figure 1.

curves obtained in the absence of electrostatic interactions. The structures in Figure 3 are numerical solutions of the elastic equations of a 1000 bp DNA rod governed by a modified Debye−Hückel repulsive force between partially neutralized point charges (corresponding to two phosphate groups with a net charge of $0.48e^-$ projected every 3.4 Å along the chain contour).[25] The supercoiled DNA configurations in Figure 4 are snapshots revealed in Brownian dynamics simulations of a sequence of DNA beads (Huang, J.; Schlick, T., unpublished results), which are modeled as interacting charged cylinders.[26] The DNA axes are described by a series of piecewise cubic B-spline curves which are guided by controlling points,[27,28] and an approximation algorithm is used to generate the coordinates of uniformly (1.7 Å) spaced point charges along these pathways.[29]

To compute the counterion binding fraction θ_z of an arbitrary configuration of DNA with N_p phosphate groups in the presence of a single species of counterion of valence z, we minimize the ionic (polyelectrolyte) free

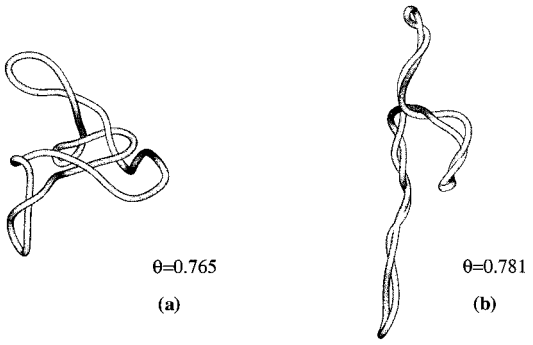

Figure 4. Sodium binding fractions θ of superhelical structures of a 3000 bp DNA plasmid with $\Delta Lk = -17.13$ at two different ionic strengths, 0.01 and 0.2 M NaCl, obtained by Brownian dynamics simulations (Huang, J.; Schlick, T. unpublished results). The bending and twisting constants are fixed at 2.0×10^{-19} erg cm and $= 3.0 \times 10^{-19}$ erg cm, respectively. The structures in panels a and b have the following characteristics, with all quantities defined in the caption to Figure 1: (a) $Wr = -6.34$, $R_g = 400.24$ Å, $\langle P-P \rangle = 1075.7$ Å; (b) $Wr = -12.42$, $R_g = 591.04$ Å, $\langle P-P \rangle = 1075.72$ Å.

energy g^{ionic} with respect to θ_z by setting $\partial g^{\text{ionic}}/\partial\theta_z = 0$. The root of this equation is given by,

$$-\frac{2zq^2(1-z\theta_z)}{N_p kT}\sum_{i<j}^{N_p}\frac{e^{-\kappa r_{ij}}}{\epsilon r_{ij}} + 1 + \ln\left(\frac{10^3\theta_z}{c_s V_z}\right) = 0 \quad (1)$$

where kT is the product of Boltzmann constant and Kelvin room temperature, ϵ is the dielectric constant of water (78.3), q is the protonic charge, c_s is the molar salt concentration, κ is the Debye–Hückel screening parameter (proportional to the square root of c_s), r_{ij} is the interphosphate distance, and $V(z)$ is the condensation volume ($V_1 = 646$ cm^3/mol of phosphate, $V_2 = 1121$ cm^3/mol of phosphate, and $V_3 = 1563$ cm^3/mol of phosphate for univalent, divalent, and trivalent counterions, respectively). The details of the derivation of eq 1 and the assumptions underlying it (e.g., delocalized mode of counterion binding, salt concentration in excess over phosphate concentration, condensation volume equal to its limiting value) are described elsewhere.[7] In practice, for a given configuration of DNA at fixed ionic conditions, the root θ_z of eq 1 is determined numerically using the Newton–Raphson method.[30]

We have also made some calculations in mixed salt systems such as NaCl/$MgCl_2$, using a straightforward numerical approach to the two-variable counterion condensation theory for counterions of mixed valence types.[6] The conclusions do not differ from what we find for counterions of a single type, and we do not show them here.

It should be noted that our calculations do not take into account any inhomogeneities of the counterion binding fraction along the length of the DNA. It is possible that regions of higher phosphate charge density condense more counterions than the locally linear parts; we report an average counterion binding fraction for the entire polymer. On the other hand, the gel mobility measurements[1–3] that have motivated our calculations also probe an average net charge. It may be, however, that this limitation of both our theory and the experiment is important (see Discussion).

3. Results

Straight Lines and Circular Arcs. We begin by reporting our results for two parallel linear DNAs, each with 2500 phosphates. For univalent counterions, analytical theory predicts that charge neutralization by counterion condensation varies from $1 - \xi^{-1}$, or 0.76, for large separation distances to $1 - (2\xi)^{-1}$, or 0.88, for small distances.[5] The numerical results listed in Table 1 confirm this prediction, but they also indicate that the small-distance limit is approached only at unrealistically short distances (but see the Discussion). For DNA, the contact distance for two segments—represented in our model by their double helical axes—is 20 Å, and at this distance, the neutralization fraction differs appreciably from an isolated single segment only at low ionic strength. It is also worth noting from Table 1 that substantial increases in charge neutralization occur only after the approaching DNAs have penetrated the Debye length of the solution (96 Å at 10^{-3} M NaCl and 9.6 Å at 10^{-1} M).

Table 1. Fractional Charge Neutralization by Univalent Condensed Counterions of Two Parallel DNA Segments, Each with 2500 Phosphates

	NaCl concentration			NaCl concentration	
d, Å[a]	0.001 M	0.1 M	d, Å[a]	0.001 M	0.1 M
1000	0.761	0.773	10	0.847	0.811
100	0.781	0.773	5	0.862	0.843
50	0.802	0.773	2	0.877	0.879
20	0.830	0.784			

[a] d = distance between segments.

Table 2. Fractional Charge Neutralization of a Circular Arc DNA Segment (84 phosphate groups) with Varying Radius of Curvature *R* in Å[a]

$1/\kappa$	$R = \infty$	$R = 1000$	$R = 400$	$R = 100$	$R = 45$	$R = 30$
961.2	0.626	0.626	0.626	0.628	0.633	0.643
304.0	0.681	0.681	0.681	0.682	0.687	0.696
96.1	0.723	0.723	0.723	0.725	0.728	0.736
30.4	0.749	0.749	0.749	0.750	0.751	0.756
9.6	0.766	0.766	0.766	0.767	0.767	0.768

[a] $1/\kappa$ = Debye screening length in Å. From top to bottom, the screening lengths correspond to NaCl molarities from 10^{-5} to 10^{-1} M in order of magnitude increments.

Since the close approach of distant segments in supercoiled DNA can occur at different contact angles, we have modeled this situation as well as a parallel approach. Our results show that the influence on charge neutralization of close approach of two segments drops off sharply as the angle of approach increases from zero (parallel segments). For instance, when two 2500 phosphate segments approach in parallel in 10^{-3} M aqueous NaCl, the charge neutralization fraction increases from 0.761 at 1000 Å separation to 0.830 at 20 Å (Table 1). But when the approach of the same segments at the same ionic strength occurs at a 20° angle, the corresponding increase of charge neutralization is only from 0.763 to 0.772.

In Table 2 we list neutralization fractions for a 42 base pair linear DNA (84 phosphate groups, length 143 Å) bent into circular arcs of varying radius of curvature R. The tightest arc, $R = 30$ Å, corresponds to about three quarters of a complete circle. Reading down any column, we see an increase in neutralization for a fixed shape as the salt concentration increases (Debye length $1/\kappa$ decreases). The increased neutralization fraction approaches the theoretical limit for long rodlike polyions, $1 - \xi^{-1} = 0.76$, when the Debye length is shorter than the length of the DNA (high ionic strength). The smaller neutralization fractions observed for longer Debye lengths (low ionic strength) is then due to end effects. Of more

interest to us here is the variation on reading along a row. For any fixed Debye length (ionic strength), the neutralization fraction increases as the circular arc becomes tighter. In all cases, however, the increase is small.

Supercoils. A closed-circular supercoiled DNA may condense more counterions than its open linear isomer due to two of its structural features, curvature and close proximity of segments. In view of Table 2, however, we expect only a slight influence of the curvature; and in view of Table 1, we expect a maximum charge neutralization fraction of about 0.83 at low ionic strengths and at higher ionic strengths a value at most only slightly higher than the value 0.76 characteristic of linear DNA. The results of our detailed calculations confirm the expectation. We look first at Figure 2, which presents the neutralization fractions in NaCl solution for the series of short supercoiled DNAs[24] illustrated in Figure 1. The spread of counterion binding fractions at low ionic strengths is from about 0.80 to about 0.83, the higher values corresponding to the more compact structures (more points of self-contact). At 0.1 M NaCl all fractions converge to about 0.78.

In Figure 3 we show a series of linear interwound forms that represent minimum-energy configurations at 0.1 M NaCl of the same 1000 bp DNA molecule but with progressively increasing linking numbers.[25] The neutralization fractions shown in the figure are clearly correlated with the increasing number of superhelical turns, but the amount of increase is very small. For these structures, more extended and representative of naturally occurring DNA supercoils than those in Figure 1, the values of the neutralization fractions are closer to the lower limit 0.76 for an open linear DNA.

Figure 4 illustrates an ionic strength transition. The configuration on the left is a structure from the dynamical equilibrium ensemble at a low ionic strength, 0.01 M NaCl.[26] The equilibrium shifts to more writhed structures at 0.2 M NaCl, typified by the form on the right.[25] The more compact high ionic strength structure is slightly but significantly more neutralized than the relatively open low ionic strength configuration.

4. Discussion

We have found a tendency for relatively compact DNA structures to condense more counterions than relatively open structures. We have also found that the increases of the counterion binding fractions are small.

The neutralization fraction by condensed sodium counterions of linear, circular, three-lobed interwound (with $\Delta Lk = 5.02$ and distance of closest approach = 20 Å, see Figure 1), and two parallel linear DNA segments separated by 20 Å, all at 10^{-3} M NaCl and with a total of 718 phosphate groups, is 0.76, 0.76, 0.83, and 0.83, respectively. Thus, the increase of sodium binding of the three-lobed interwound superhelix relative to the linear and circular forms of DNA is significant and is the same as that of two parallel segments separated by the contact distance of 20 Å. On the other hand, at NaCl concentrations approaching physiological (about 0.1−0.2 M) and in $MgCl_2$ or $NaCl/MgCl_2$ solutions of any ionic strength (not shown), the phosphate charge neutralization is almost the same for all these different DNA configurations.

For a series of linear interwound superhelical structures (Figure 3) with an increasing number of superhelical turns (each is an equilibrium structure at 0.1 M NaCl for a specified linking number), we calculate sodium binding fractions that increase with increased winding. The increase, however, is in the third decimal place, and to two places, all neutralization fractions are equal to 0.78. Even in panel d of Figure 3, which shows an interwound shape with an extended region of self-contact, the binding fraction does not exceed (to two decimal places) the value for the open circle in panel a. It should be noted, however, that "self-contact" here does not correspond to the steric limit 20 Å. The greater distances of closest approach (40−55 Å) reflect repulsive electrostatic forces that prevent DNA segments from touching each other in an equilibrium structure. It may also be useful to point out that when the systematic increase in the third decimal place of the neutralization fractions is translated into a number of condensed counterions (see below), we do find that the most tightly wound structure, panel d, binds 12 more counterions than the open circle in panel a.

Increased screening of repulsions among phosphate groups causes an equilibrium superhelical configuration to become more compact at higher ionic strengths. The shift of the same closed-circular DNA molecule from the low-salt (0.01 M NaCl) equilibrium form in panel a of Figure 4 to the high-salt (0.2 M) equilibrium shape in panel b is accompanied by a modestly increased phosphate charge neutralization fraction from 0.765 to 0.781. Although the percentage increase is slight, it does mean that there is an uptake of about 96 sodium ions by the 6000 phosphate charges on the DNA. If these additional sodium ions were localized to the regions of relatively close approach (there are about 10 of them) in the high-salt shape of panel b of Figure 4, then sodium ion uptake could provide a significant driving force for compaction. Our calculations unfortunately cannot make such a prediction, because we can compute only a uniform average increase of neutralization fraction along the entire chain. Confident detection of condensed counterion inhomogeneities along the polymer may require all-atom modeling. On the other hand, an increased average value is obviously caused in our computation by regions of closer approach of the polymer charges.

To our knowledge, only Ma and Bloomfield[1] have attempted to measure the extent of phosphate neutralization by condensed counterions for DNA supercoils. They were able to detect no significant differences for open linear and closed-circular supercoiled DNA. Their study was not a systematic exploration of the possibilities, however. Only a small number of ionic conditions were utilized, and the supercoiled configurations were not systematically varied. On the other hand, their method (gel electrophoresis) produces high-precision data, and the interpretation of their primary data has theoretical support. Since we have found a small but clear correlation of ion binding with increased DNA supercoiling, there might be some interest in a more extensive experimental program dedicated to this aspect of DNA electrostatics.

Acknowledgment. This work was supported in part by the U.S. Public Health Service under grants GM34809 (W.K.O.) and GM36284 (G.S.M.). Calculations were performed at the Rutgers University Center for Computational Chemistry. We are grateful to David Swigon, Tim Westcott, and Tamar Schlick for providing the coordinates used in the supercoiled DNA structures. We

thank David Swigon as well for help in the use of Tecplot and discussion of our results.

References and Notes

(1) Ma, C.; Bloomfield, V. A. *Biopolymers* **1995**, *35*, 211−216.
(2) Li, A. Z.; Qi, L. J.; Shih, H. H.; Marx, K. A. *Biopolymers* **1996**, *38*, 367−376.
(3) Li, A. Z.; Huang, H.; Re, X.; Qi, L. J.; Marx, K. A. *Biophys. J.* **1998**, *74*, 964−973.
(4) Li, A. Z.; Marx, K. A. *Biophys. J.* **1999**, *77*, 114−122.
(5) Ray, J.; Manning, G. S. *Langmuir* **1994**, *10*, 2450−2461.
(6) Manning, G. S. Q. *Rev. Biophys.* **1978**, *11*, 179−246.
(7) Fenley, M. O.; Manning, G. S.; Olson, W. K. *Biopolymers* **1990**, *30*, 1191−1203.
(8) Adrian, M.; ten Heggeler-Bordier, B.; Wahli, W.; Stasiak, A. Z.; Stasiak, A.; Dubochet, J. *EMBO J.* **1990**, *9*, 4551−4554.
(9) Bednar, J.; Furrer, P.; Stasiak, A. Z.; Dubochet, J.; Egelman, E. H.; Bates, A. *J. Mol. Biol.* **1994**, *235*, 825−847.
(10) Fenley, M. O.; Olson, W. K.; Tobias, I.; Manning, G. S. *Biophys. Chem.* **1994**, *50*, 255−271.
(11) Schlick, T.; Li, B.; Olson, W. K. *Biophys. J.* **1994**, *67*, 2146−2166.
(12) Vologodskii, A. V.; Cozzerelli, N. R. *Annu. Rev. Biophys. Biomol. Struct.* **1994**, *23*, 609−643.
(13) Vologodskii, A. V.; Cozzerelli, N. R. *Biopolymers* **1995**, *35*, 289−296.
(14) Gebe, J. A.; Delrow, J. J.; Heath, P. J.; Fujimoto, B. S.; Stewart, D. W.; Schurr, J. M. *J. Mol. Biol.* **1996**, *262*, 105−128.
(15) Lyubchenko, Y. L.; Shlyakhtenko, L. S. *Proc. Natl. Acad. Sci.* U.S.A. **1997**, *94*, 496−501.
(16) Delrow, J. J.; Gebe, J. A.; Schurr, J. M. *Biopolymers* **1997**, *42*, 455−470.
(17) Hammermann, M.; Steinmaier, C.; Merlitz, H.; Kapp, U.; Waldeck, W.; Chirico, G.; Langowski, J. *Biophys. J.* **1997**, *73*, 2674−2687.
(18) Jayaram, B.; Swaminathan, S.; Beveridge, D. L.; Sharp, K.; Honig, B. *Macromolecules* **1990**, *23*, 3156−3165.
(19) Deserno, M.; Holm, C.; May, S. *Macromolecules* In press.
(20) Fenley, M. O.; Manning, G. S.; Olson, W. K. *J. Phys. Chem.* **1992**, *96*, 3963−3969.
(21) Fixman, M. *J. Chem. Phys.* **1990**, *92*, 6283−6293.
(22) Chandrasekaran, R.; Arnott, S. In *Landolt-Börnstein Numerical Data and Functional Relationships in Science and Technology, New Series, Group VII: Biophysics, Volume 1, Nucleic Acids, Subvolume b, Crystallographic and Structural Data*; Saenger, W., Ed.; Springer-Verlag: Berlin, 1989; p 31.
(23) El Hassan, M.; Calladine, C. R. *Trans. R. Soc. London A* **1997**, *355*, 43−100.
(24) Coleman, B. D.; Swigon, D.; Tobias, I. *Phys. Rev. E* In press.
(25) Westcott, T. P.; Tobias, I.; Olson, W. K. *J. Chem. Phys.* **1997**, *107*, 3967−3980.
(26) Jian, H.; Schlick, T.; Vologodskii, A. *J. Mol. Biol.* **1998**, *284*, 287−296.
(27) Hao, M.-H.; Olson, W. K. *Biopolymers* **1989**, *28*, 873−900.
(28) Hao, M.-H.; Olson, W. K. *Macromolecules* **1989**, *22*, 3292−3303.
(29) Fenley, M. O.; Olson, W. K.; Chua, K.; Boschitsch, A. H. *J. Comput. Chem.* **1996**, *17*, 976−991.
(30) Press, W. H.; Flannery, B. P.; Teukolsky, S. A.; Vetterling, W. T. *Numerical Recipes. The Art of Scientific Computing*; Cambridge University Press: Cambridge, 1989; pp 254−259.

MA990191U